Link Analysis of a Telecommunication System on Earth, in Geostationary Orbit, and at the Moon: Atmospheric Attenuation and Noise Temperature Effects

C. Ho,[1] A. Kantak,[1] S. Slobin,[2] and D. Morabito[1]

Two uncertain factors affecting a telecommunication system's performance are effective antenna gain and system noise temperature. For an Earth-geostationary satellite–Moon system, they are attributed to the atmospheric attenuation and radiation. In the super-high frequency band, the attenuations are mostly weather related and have the same values for both upward- and downward-propagating signals, while brightness temperatures have different effects for upward- and downward-looking antennas. In this study, six link scenarios for this system are analyzed. Analysis of atmospheric attenuation and brightness temperatures for each link are presented. This study also discusses the general methodology for determining the noise temperature for a receiving antenna pointing to a blackbody of a given angular extent. A set of curves is presented that is independent of the sizes and brightness temperatures of black bodies. Antenna noise temperature increases are calculated as a function of distance between the antenna beam center and the blackbody disk center normalized by the disk radius. To show an example, these ratios are applied to a case of an Earth-based antenna looking toward the Moon.

I. Introduction

In the coming decade, NASA is planning to send missions to the Moon. To carry out each mission successfully, high quality Earth–Moon telecommunication will be crucial. To have a robust link between the ground and the spacecraft either on the Moon or in orbit around it, one needs to accurately characterize the communications channel between the transmitter and the receiver. This is especially true for high-capacity links that will be required in the future. There are two major areas in the characterization of the communications channel that need to be better understood: the first area is the various effects of the Earth's atmosphere that produce attenuation by absorbing or scattering the radio signals that pass through it, and the second, equally important area is the system noise temperature increase at the

[1] Communications Architectures and Research Section.

[2] Communications Ground Systems Section.

The research described in this publication was carried out by the Jet Propulsion Laboratory, California Institute of Technology, under a contract with the National Aeronautics and Space Administration.

receiving end of the link due to the Moon and the Earth acting as hot bodies. This study will determine the effects of the two parameters as accurately as possible.

It is well-known that the degradations induced by the Earth's atmosphere and weather are rather severe for transmissions in the super-high frequency band (SHF = 3 to 45 GHz) as compared with lower frequency bands [1,2].[3,4] To utilize a highly sensitive communications system such as the Deep Space Network (DSN) system maximally in terms of data rates, the atmospheric effects must be understood thoroughly. As an example, for the link to work with acceptable margins at the receiver (e.g., 3 dB) 99 percent of the time in a year, appropriate values of loss due to the atmosphere will be needed along with the system noise temperature increase numbers when the angularly extended Moon is within the DSN antenna beam. These link degradation effects are addressed below.

Any natural absorbing medium in the atmosphere that interacts with the transmitted radio wave will not only produce signal attenuation [3–5], but will also be a source of radiated thermal noise power [6,7]. Thus, the effects of atmosphere and weather on super-high frequency (SHF) signals are like a double-edged sword. On one hand, atmosphere and weather phenomena such as clouds, fog, and rain can cause attenuation of microwaves through absorption, resulting in a reduction of the receiving system's effective gain, G. On the other hand, these media radiate radio noise to the background, causing an increase in the system noise temperature, T. As a final result, the G/T ratio of the receiving system will decrease due to both effects [1,2].[5]

At frequencies below 1 GHz, radio noise caused by atmospheric radiation is less than a few kelvins. This is negligible when compared with a receiving system with a noise temperature of several tens or a hundred kelvins. However, at frequencies above 1 GHz, the radio noise caused by atmospheric emission increases significantly with increasing frequency [8,9]. At some frequencies and antenna elevation angles, the noise temperature can be as high as 300 K. This background temperature cannot be neglected and needs to be considered in the receiving system design.

There are several sources that contribute radio noise at the SHF band. For an Earth-based downlink, when a low-noise receiver receives an SHF band signal from a spacecraft, at the same time it also receives noise from the sources shown in Fig. 1. These include the cosmic background radiation (2.7 K), galactic noise, and emissions from atmospheric gases (oxygen and water vapor), clouds and rain, the surface of the Earth (ground pickup through side lobes), and the Sun and Moon, etc. For an uplink, the spacecraft receives SHF signals from the ground transmitter and also upward noise emissions from atmospheric gases, clouds and rain,[6,7] and the Earth's surface (including land, bodies of water, ice, and vegetation).

In this study, we will estimate the signal attenuation and system noise temperature for various telecommunication links by including all contributions of signal attenuation and noise. These include Earth–geostationary satellite, Earth–Moon, and geostationary satellite–Moon uplinks and downlinks. Here we have assumed that a geostationary satellite can point its antenna and communicate in any direction, including the Earth and Moon. In the following sections, the fundamental theory and six cases of link analyses for an Earth–geostationary satellite–Moon telecommunication system are presented.

---

[3] C. Ho, C. Wang, K. Angkasa, and K. Gritton, *Estimation of Microwave Power Margin Losses Due to Earth's Atmosphere and Weather in the Frequency Range of 3–30 GHz*, JPL D-27879 (internal document), Jet Propulsion Laboratory, Pasadena, California, January 2004.

[4] C. Ho, S. Slobin, and K. Gritton, *Atmospheric Noise Temperature Induced by Clouds and Other Weather Phenomena at SHF Band (1–45 GHz)*, JPL D-32584 (internal document), Jet Propulsion Laboratory, Pasadena, California, August 2005.

[5] Ibid.

[6] C. Ho, *Attenuation/Scintillation Effects on Ka-Band Signals due to Clouds: Experimental and Theoretical Studies*, JPL D-33750 (internal document), Jet Propulsion Laboratory, Pasadena, California, November 20, 2005.

[7] K. Gritton, C. Ho, and R. Crane, *Ka-Band Propagation Model Based on High Resolution ACTS Data*, JPL D-30175 (internal document), Jet Propulsion Laboratory, Pasadena, California, August 20, 2004.

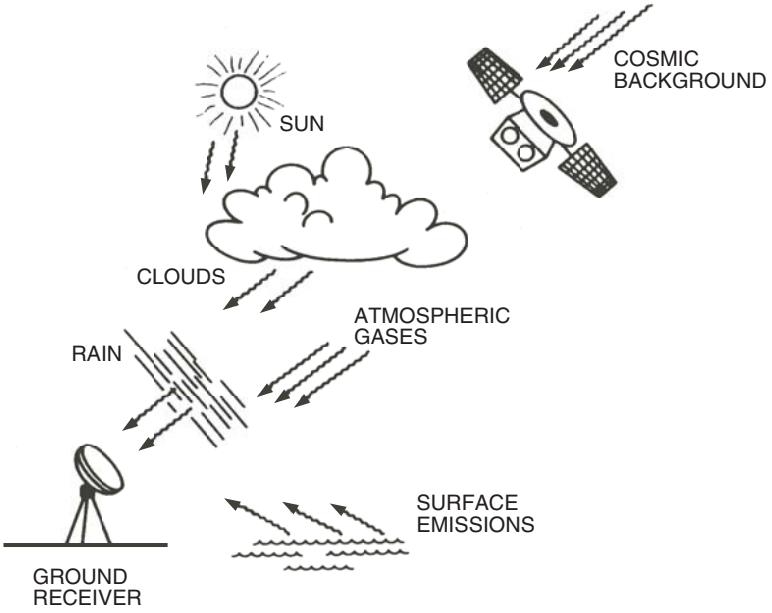

Fig. 1. An illustration of a generic communications link from a spacecraft to a ground receiver.

II. Fundamental Theory

A. Ratio of $G_{\text{eff}}/T_{\text{op}}$

The data rate of a communications link is a function of many parameters of the link, namely, the distance between the transmitter and receiver (that is, range), the effective isotropically radiated power (EIRP) of the transmitter, the transmitting and receiving antenna pointing accuracy, the receiving antenna gain, other transmitting and receiving system losses, the atmospheric losses of the channel, and finally the system noise temperature of the receiver [1,2].[8] It is customary to define the performance of the receiver system by the ratio of the total effective gain of the receive antenna, G_{eff}, to the total operating system noise temperature, T_{op}. The effective gain of an antenna is the gain available after all losses are deducted from the gain of the antenna, and T_{op} is the sum of all noise temperature contributions, such as from the amplifier and follow-on equipment temperature, antenna temperature, background temperature, etc. The ratio of energy per bit received by the receiver to the thermal noise power spectral density, i.e., the received E_b/N_o, is sometimes used as the performance measure for the link because the data link margin depends upon it. It should be noted that the noise power spectral density, N_0, is the product of the operational total system noise temperature, T_{op}, and Boltzmann's constant (1.38×10^{-23} J/K = -228.6 dBW/K/Hz). Furthermore, E_b/N_o is proportional to the ratio of the receiving antenna, $G_{\text{eff}}/T_{\text{op}}$. The following formulas give the G_{eff} and T_{op} for a link:

$$\begin{aligned} G_{\text{eff}}\ (\text{dBi}) &= G_{\text{vac}}\ (\text{dBi}) - A_{\text{atm}}\ (\text{dB}) \\ T_{\text{op}}\ (\text{K}) &= T_{\text{vac}}\ (\text{K}) + T_{\text{bg}}\ (\text{K}) \end{aligned} \tag{1}$$

where G_{vac} is the antenna gain in a vacuum, A_{atm} is the loss endured by the propagating signal through the atmosphere in the vicinity of the antenna along the signal path, including the propagation loss (space

[8] C. Ho et al., op cit., 2005.

loss), $T_{\rm vac}$ is the system's vacuum noise temperature, and $T_{\rm bg}$ is the receiving antenna noise temperature after coupling with the background noise brightness temperature. The background noise temperature has several components, as shown in Fig. 1. It should be noted that the emissions from atmospheric gases, clouds, rain, the Earth's surface, the Sun, and cosmic background radiation, along with the radiated and reflected emissions from the ground in the vicinity of the antenna site, are the noise components received by an upward-looking antenna, causing the increase of noise temperature in the receiver.

The change of G/T ratio with respect to a vacuum condition is given by

$$\Delta(G/T)_{\text{w.r.t. vacuum}} = -A_{\rm atm}\ (\text{dB}) - 10 \times \log_{10}\left[\frac{T_{\rm vac} + T_{\rm bg}}{T_{\rm vac}}\right] \tag{2}$$

where the loss is assigned a minus sign indicating that an increase in either $A_{\rm atm}$ or $T_{\rm bg}$ or both will cause a decrease of G/T. For a system with low receiving system noise temperature (i.e., a low $T_{\rm vac}$), the $T_{\rm bg}$ contribution is the most significant source of loss in G/T.

B. Background Noise Temperature

The noise power received by a receiving station antenna due to a hot body at a given frequency usually is expressed in terms of the body's brightness temperature, or noise temperature. The brightness temperature of a source (hot body) is a measure of the power radiated in a given frequency band by the source in the direction of the receiving antenna. This is equal to the physical temperature of a blackbody (perfect absorber) emitting the same power in that band [10].

In general, the noise power received by an antenna is the sum of the emitted power of the source in the direction of the antenna within the frequency band of interest and the power from the surrounding medium that is reflected by objects or reflecting surfaces toward the antenna. These power contributions are further attenuated by the medium present between the antenna and the reflecting surfaces. The brightness temperature is a background temperature in a certain direction and is independent of the receiving antenna vacuum system noise temperature or the antenna gain. The radio noise emitted from the atmosphere in thermodynamic equilibrium, from Kirchoff's Law, is equal to its absorption, and this equality holds for all frequencies. The brightness temperature, T_b (in astronomy [10,11] referred to as the background temperature observed by a ground antenna in a given direction through the atmosphere), in a fixed frequency band is given by radiative transfer theory [3]:

$$T_b = \int_0^\infty T(l)\kappa(l)e^{-\tau(l)}dl + T_\infty e^{-\tau_\infty} \tag{3}$$

where the optical depth is

$$\tau(l) = \int_0^l \kappa(l')dl' \tag{4}$$

which is an integral along the path, l, from a radiating parcel to the ground; $d\tau(l) = \kappa(l)dl$, where $\kappa(l)$ is the absorption coefficient, a function of atmospheric species, its abundance, temperature, pressure, height, and the frequency; and T_∞ is the cosmic background noise temperature from infinity with an optical depth τ_∞. For a homogeneous, isothermal atmosphere, $\kappa(l) = \kappa$, the mean absorption coefficient, and $T(l) = T_m$, the mean physical temperature. Thus, the optical depth through the total path is $\tau(l) = \kappa l$. Equation (3) becomes

$$T_b = T_m \int_0^{l_0} e^{-\kappa l} \kappa dl + T_\infty e^{-\tau_\infty} \tag{5}$$

where the integration covers all radiative atmospheric elements from the ground to the top of the atmosphere l_0, T_m is the physical temperature of the medium, κ is the absorption coefficient, and τ is the optical depth to the point under consideration. There is a relation between the τ and the attenuation, A (in dB), due to the gaseous absorption over the path. At the SHF band, the last term in the above equation reduces to 2.7 K, and the cosmic background component (unless the Sun or the Moon or both are in the beamwidth of the antenna) can be neglected.

C. Noise Temperature and Attenuation

Performing the integration indicated in Eq. (5), the brightness temperature is further reduced to [1,2][9]

$$T_b = T_m(1 - e^{-\tau_0}) = T_m(1 - e^{-\kappa l_0}) = T_m(1 - 10^{-(A(\text{dB})/10)}) = T_m \left(1 - \frac{1}{L}\right) \text{ (K)} \tag{6}$$

where $\tau_0 = \kappa l_0$ is the total optical depth for the atmosphere and $L = e^{\tau_0} = e^{\kappa l_0} = e^{A/4.34} = 10^{A/10}$ is a linear loss factor due to the atmospheric absorption. We can see that, when L becomes very large, T_b equals T_m. Thus, T_m is the upper limit of T_b. The attenuation in decibels of a lossy medium can be calculated from the loss factor L as

$$A = 10 \log_{10} L \text{ (dB)} \tag{7}$$

The mean ambient temperature, T_m, ranges from about 260 to 280 K on Earth, depending mostly on the height above the surface of the primary radiating atmospheric component. For example, water vapor is concentrated primarily close to the Earth's surface, so its mean physical temperature is somewhat higher than that of the oxygen component. Thus, Eq. (6) sets up the relationship between the attenuation caused by the atmospheric absorption at any height and the brightness temperature due to the radiation.

Using $T_m = 275$ K, we find that the noise temperature rises quickly with the atmospheric attenuation level. It is 56 K for 1-dB attenuation, 137 K for 3-dB attenuation, and 188 K for 5-dB attenuation. There is a further relationship that determines the value of T_m from the surface temperature, T_s, measured when a total zenith atmospheric attenuation is fixed:

$$T_m = 1.12T_s - 50 \text{ (K)} \tag{8}$$

The flat-Earth approximation is often used to calculate atmospheric attenuation at elevation angles other than at zenith. Given the zenith atmospheric loss, L_0 or A_0 (dB), for a horizontally stratified atmosphere, then

$$A(\theta) = \frac{A_0}{\sin\theta} \tag{9}$$

and

$$L(\theta) = L_0^{1/\sin\theta} \tag{10}$$

[9] Ibid.

The brightness temperature at an elevation angle θ is given by

$$T_b(\theta) = T_m \left(1 - 10^{-A_0(\text{dB})/(10 \sin\theta)}\right) = T_m \left(1 - 1/L_0^{1/\sin\theta}\right) \tag{11}$$

For elevation angles greater than 30 deg, the error using Eq. (11) as compared with round-Earth ray-path calculations is much less than 1 percent of the total values [5]. This equation can be used quite accurately for brightness temperature estimates down to an elevation angle of 10 deg, with an error of less than 2 percent of the values.

D. Noise Figure and Antenna Noise

There are two common parameters that are most useful for communication system performance evaluation: noise figure, F_a in decibels, and noise temperature, T_a in kelvins. Noise figure and noise temperature are related by the following equation [6,10]:

$$F_a = 10 \log_{10} \left(1 + \frac{T_a}{T_0}\right) \text{ (dB)} \tag{12}$$

where T_0 is the ambient reference temperature of 290 K.

Figure 2 summarizes the median expected noise levels produced by sources of external radio noise in the frequency range applicable to practical space communications [6,7]. Noise levels are expressed in terms of both noise temperature, t_a (right vertical axis), and noise figure, F_a (dB) (left vertical axis). The noise

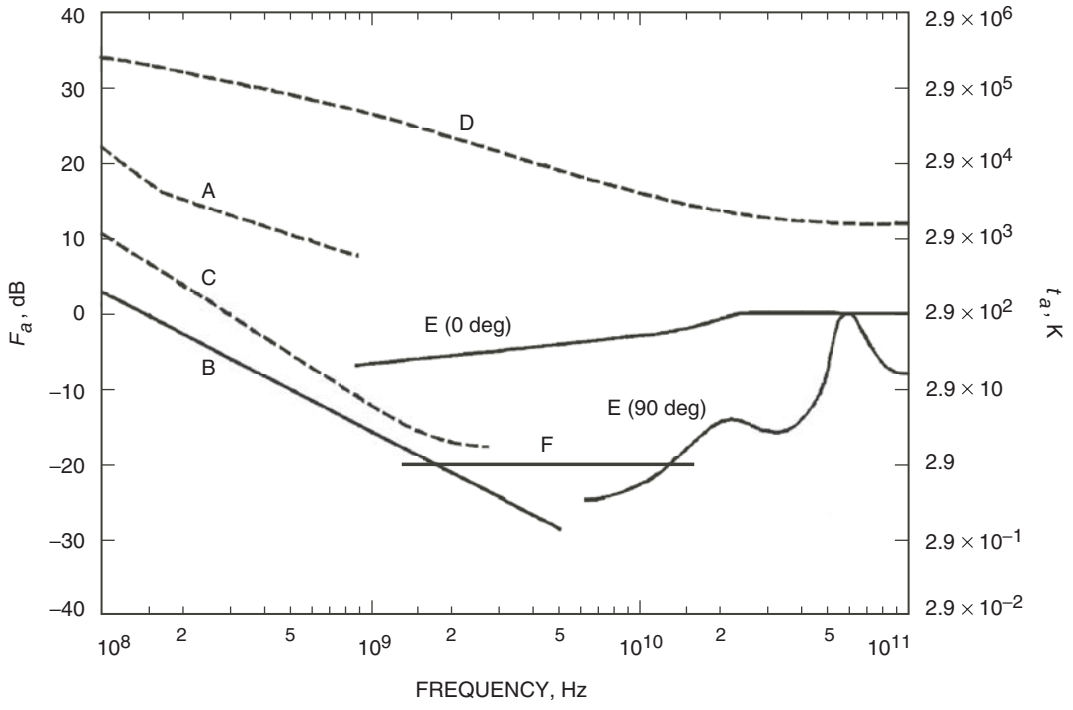

Fig. 2. External noise figure F_a (dB) and sky temperature t_a (K) versus frequency (0.1 to 100 GHz): Plot A, estimated man-made noise on Earth; B, galactic noise; C, galactic noise (toward the galactic center with infinitely narrow beamwidth); D, quiet Sun (0.5-deg beamwidth directed at the Sun); E, Earth atmospheric radiation, 0- to 90-deg elevation angles; and F, blackbody (2.7-K) radiation [6].

contributions from atmospheric gaseous noise at elevation angles of 0 and 90 deg [curves E(0 deg) and E(90 deg)] are shown. We can see that above 1 GHz the absorptive constituents of the atmosphere, i.e., oxygen, water vapor, and rain (curves E), act as the dominant noise sources and can reach a maximum value of 290 K under extreme conditions. The Sun is a strong variable noise source, reaching values of 10,000 K and higher when observed with a narrow-beamwidth (<0.5 deg) antenna directed at the Sun (curve D), under quiet Sun conditions. The cosmic background noise level of 2.7 K (curve F) is very low and is not a significant noise contributor in space communications.

Antenna thermal noise is conveniently treated in terms of noise temperature, since the two parameters are linearly related. In circuit theory, the noise power, p_n, that is transferred to a matched load is expressed as

$$P_n = k_B T_n B \text{ (watts)} \tag{13}$$

where k_B is Boltzmann's constant, T_n is antenna noise temperature in kelvins, and B is the bandwidth in hertz. Thermal radiation power flux from gaseous atmosphere is given by the Rayleigh–Jeans approximation to Planck's equation:

$$P_n = \frac{2k_B T}{\lambda^2} = 22.2 k_B T f^2 \text{ (watts/Hz/m}^2\text{/rad}^2\text{)} \tag{14}$$

where f is the frequency in gigahertz.

III. Telecommunication Link Analysis

A. Earth-Based Antenna Pointing to a Spacecraft

The spacecraft mentioned here can be a low Earth-orbit satellite, a geostationary satellite, or a deep-space spacecraft. When performing the link analysis, uncertainties in background noise temperature and atmospheric attenuation are usually the two dominant parameters in the link performance. The background noise temperature coupled to a receiving antenna is usually taken into account as the antenna noise temperature contribution term that is a part of the system operating noise temperature, while atmospheric attenuation results in a reduced effective antenna gain reduction.

1. Antenna Noise Temperature. For a spacecraft-to-Earth-based antenna downlink, the ground station antenna tracks the spacecraft located in some orbit around the Earth or in deep space. The ground-based receiving antenna usually has its main beam pointed toward the spacecraft to optimize the signal power received from the spacecraft. However, this main lobe also picks up the atmospheric noise sources discussed above and any hot-body radiations that may be within the main-lobe beamwidth. In addition, the side lobes of the antenna also pick up the noise sources from all around the antenna site and from where the side lobes may be pointed in space. Thus, the noise sources may or may not be in the direct line of sight between the spacecraft and the receiving antenna, yet they may affect the performance of the link, depending upon the receiving antenna gain pattern. Thus, the elevation angle of the receiving antenna plays an important role in the noise received by the receiver. At high antenna elevation angles, most of the significant side lobes of the antenna will be pointed to the sky, and hence the thermal noise emission from the Earth or reflections from the Earth may be intercepted only by low-gain side lobes, producing a minimal increase of the system noise temperature. As the elevation angle decreases, e.g., when tracking a satellite near the antenna station horizon, the main lobe itself may pick up significant contribution to the system noise temperature from the thermal noise and reflections from the Earth's surface.

The antenna temperature is the weighted average of the antenna gain and the brightness temperature over the sky and ground, as shown in Fig. 3. It depends mainly on the antenna gain and brightness temperature in the pointing direction. For an antenna pointing to a direction (θ_0, ϕ_0), its received noise temperature, $T_r(\theta_0, \phi_0)$ is [12]

$$T_r(\theta_0, \phi_0) = \frac{1}{4\pi}\left[\int\limits_{\Omega \in \text{main lobe}} G_r(\theta, \phi) \cdot t_b(\theta, \phi) d\Omega + \int\limits_{\Omega \in \text{side lobe}} G_r(\theta, \phi) \cdot t_b(\theta, \phi) d\Omega\right] \tag{15}$$

where

$G_r(\theta, \phi) =$ receiver's antenna gain (dimensionless)

$T_b(\theta, \phi) =$ brightness temperatures (K) at directions (θ, ϕ)

$d\Omega =$ solid angle ($\int_\Omega d\Omega = \int_0^\pi \int_0^{2\pi} \sin\theta d\theta d\phi = 4\pi$) and $\frac{1}{4\pi}\int_\Omega G_r(\theta) d\Omega = 1$

$\theta =$ polar angle (0 to 180 deg)

$\phi =$ azimuth angle (0 to 360 deg)

In Fig. 3, T_{sky} is extra-terrestrial noise temperature from cosmic background and T_a is background temperature from atmospheric radiation with an optical depth τ from an atmospheric parcel, while T_{surf} are emissions from Earth's surface (land, water, ice, vegetation, etc.). All three types of temperatures contribute to the brightness temperature, $t_b(\theta, \phi)$, to an upward-looking antenna. The integration is over the entire sphere and includes the antenna's main beam as well as the side lobes. For an upward-looking antenna, downwelling brightness temperature is expressed as [7]

$$T_{B_d} = T_{\text{sky}} e^{-\tau} + T_a(1 - e^{-\tau}) \tag{16}$$

For a downward-looking antenna, the upwelling brightness temperature, including reflection from the surface, is

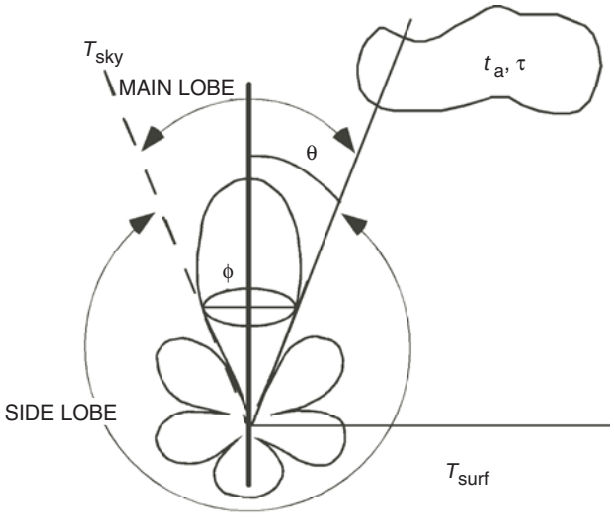

Fig. 3. Radio emission seen by an Earth-based upward-looking beam antenna.

$$T_{B_u} = \varepsilon T_s e^{-\tau} + T_a(1 - e^{-\tau}) + T_{B_d}(1 - \varepsilon)e^{-\tau} \tag{17}$$

where

$\varepsilon =$ surface emissivity, a function of frequency also depending on surface soil type, roughness, dielectric constant, moisture, etc. $(0 \leq \varepsilon \leq 1)$

$T_s =$ surface physical temperature (averages of 215 K on Mars, 300 K on Earth)

$\tau =$ atmosphere optical depth, a function of frequency and elevation angle, depending on cloud amount, gaseous absorption, etc. (a nearly transparent object has a very small τ)

$T_a =$ mean physical temperature of the atmosphere (averages of 200 K on Mars, 230 K on Earth)

$T_{\text{sky}} =$ sky temperature as a function of frequency

Noise from individual sources, such as atmospheric gases, the Sun, the Earth's surface, etc., is usually given in terms of their brightness temperatures. Figure 4 shows atmospheric noise temperatures as a function of frequency with various elevation angles for an average absolute humidity (AH = 7.5 g/m^3). The values are calculated using a median water vapor density and a standard atmosphere pressure ($P =$ 1013 mb) and International Telecommunication Union (ITU) model [1,2].[10] Figure 5 shows the cloud effects on noise temperature. The values are calculated using a moist atmosphere plus a cloud with 3-km thickness [1,2].[11] Below the 10-deg elevation angle, a round Earth model has been used for calculation. For these cases, brightness temperature will play a dominant role only in the direction of the main beam of the receiving antenna. For antennas whose gain patterns encompass a single distributed noise source (such as the Moon), the antenna temperature and brightness temperature are almost the same [1,2].[12]

2. Atmospheric Attenuations. Atmospheric attenuation values also depend on signal frequency, elevation angles, water vapor density, cloud liquid water contents, and radio climatic zone (rainfall rate). For a path other than zenith, attenuation values should be divided by a factor of $\sin\theta$, where θ is the elevation angle and 10 deg $< \theta <$ 90 deg. For a DSN site such as Goldstone, which is located in rainfall zone E, at 5 percent of the time exceeded (corresponding to a 95 percent link availability), the surface water vapor density is 12 g/cm^3, the rainfall rate is 1.0 mm/h, and the columnar content of cloud liquid water is 0.3 kg/m^2. We can apply these parameters to the four types of attenuations:

(1) Gaseous oxygen and water vapor. At an average condition, the dominant attenuation is due to atmospheric absorptions caused by oxygen and water vapor [3–5,13]. Below the 22.3-GHz water absorption line, the atmospheric absorption increases as the signal's frequency increases. At 15 GHz, the oxygen absorption can generate an attenuation of 0.05 dB for a zenith path. At the same time, the water vapor density of 7.5 g/cm^3 at the surface (average situation) can also cause an attenuation of 0.05 dB. Thus, the total zenith attenuation (oxygen plus water vapor) is typically 0.1 dB for a clear-air atmosphere. When the surface water vapor density is 12 g/cm^3 (worst case), the attenuation due to water absorption alone is typically 0.08 dB. While the oxygen absorption does not change, the total zenith attenuation is at 0.13 dB. At a 20-deg elevation angle, total atmospheric absorption is about 0.4 dB. Figure 6 shows zenith gaseous absorption for a water vapor density of 12 g/m^3, which is based on an ITU model [1,2].[13]

[10] Ibid.

[11] Ibid.

[12] Ibid.

[13] Ibid.

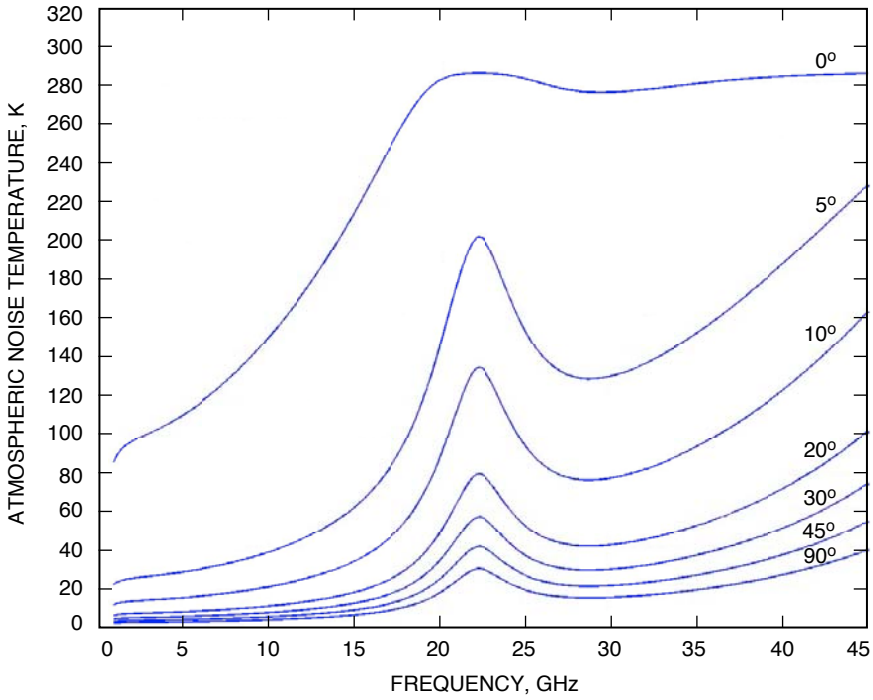

Fig. 4. Atmospheric noise temperature as a function of frequency for a clear atmosphere with various elevation angles. A median level of water vapor density (AH = 7.5 g/m^3) is applied here. At a 0-deg elevation angle, the noise temperature reaches 280 K at 20 GHz [1,2, and footnote 4].

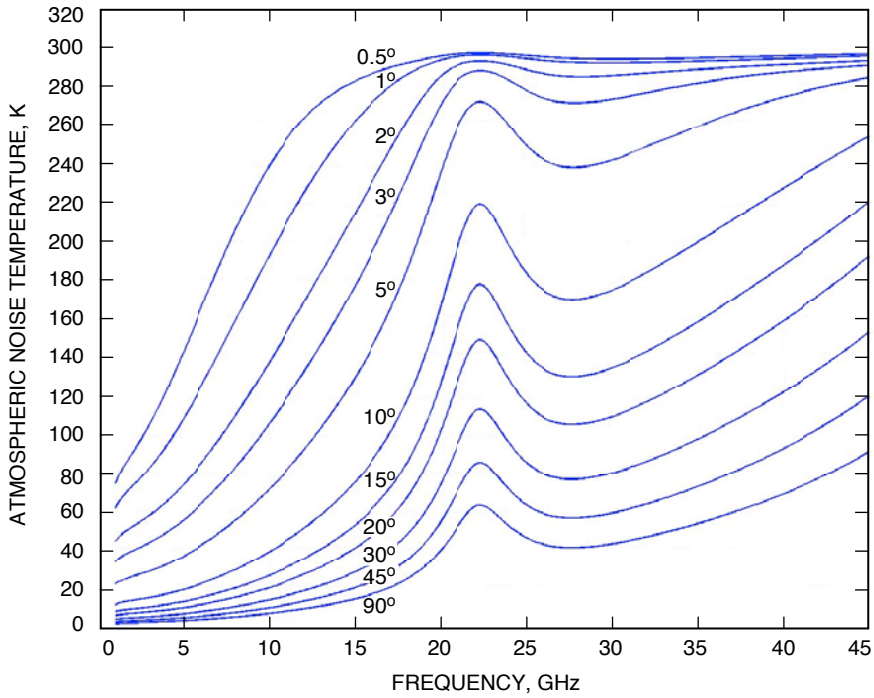

Fig. 5. Atmospheric noise temperature as a function of frequency for various elevation angles for clear air plus clouds for rainfall region E. A moist atmosphere with water vapor density of 15 g/m^3 and moderate cloud columnar liquid water content of 0.5 kg/m^2 (both at 1 percent of time exceeded) are used for the calculation [1,2, and footnote 4].

(2) Attenuation due to rain. This is the severest attenuation at this frequency range.[14] The rain attenuation is highly dependent on the rainfall rate. The attenuation increases rapidly as the frequency increases. For a path with a 20-deg elevation angle at 5.0 percent of the time exceeded, the attenuation is about 0.7 dB at 15 GHz. This means that for 95 percent of the time the attenuation is less than 0.7 dB at Goldstone.

(3) Cloud and fog attenuations. At 5.0 percent of the time exceeded, the cloud attenuation at this frequency for a zenith path is approximately 0.4 dB.[15] However, clouds can also radiate radio noise. The heavy cloud radiation can cause an increase of the receiver's system noise temperature by as much as 40 K. Thus, the increases in both signal loss and noise temperature have a dual effect on the G/T of the receiver for a low-noise receiving system.

(4) Scintillation at low elevation angle. When the microwave signal passes through a randomly fluctuating atmospheric medium, changes in the refractive index will cause scintillation in both amplitude and phase.[16] These effects become more severe with decreasing elevation angle. At a 20-deg elevation angle, the amplitude attenuation is about 0.2 dB at 15 GHz, while angle-of-arrival fluctuation due to phase scintillation is about 2 mdeg. The total margin required is 1.7 dB. Depolarization due to ice and rain has minor effects at this frequency band. However, a large antenna aperture will have smoothing effects on these degradation phenomena.

Table 1 lists the various propagation impairments for various frequency bands for a selected link availability of 95 and 99 percent at Goldstone.

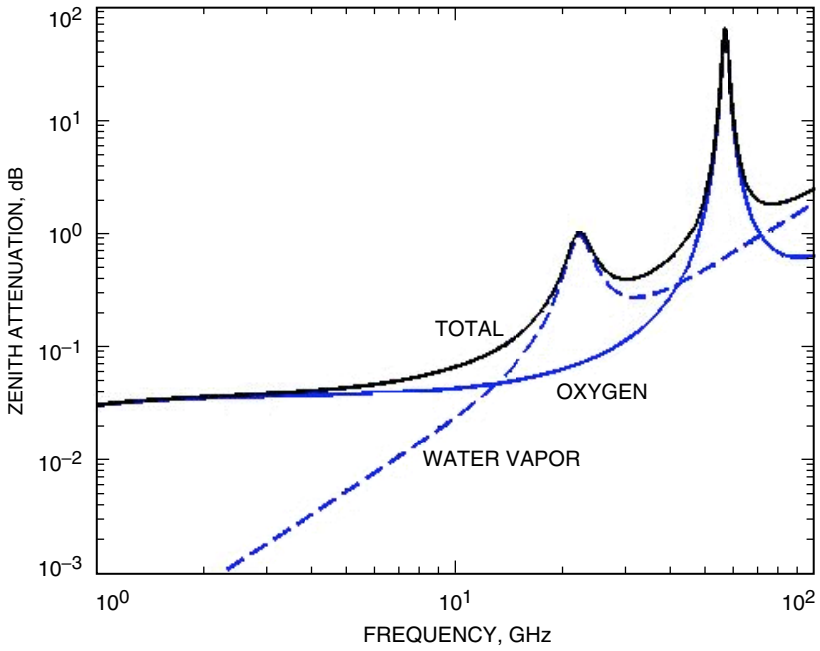

Fig. 6. Zenith gaseous absorption due to oxygen and water vapor as a function of frequency for Goldstone. A water vapor density of 12 g/m^3 is used here, corresponding to about 1 percent of time exceeded [1,2, and footnote 4].

[14] K. Gritton et al, op cit., 2004.

[15] C. Ho, op cit., 2005.

[16] C. Ho et al., op cit., 2004.

Table 1. Atmospheric attenuation for a ground–space path with a 20-deg elevation angle at Goldstone, California.

Percentage of link availability	Frequency band, GHz	Atmospheric absorption ($\rho_v = 12$ g/cm^3), dB	Rain attenuation, dB	Cloud, fog attenuation, dB	Scintillation/ multipath, dB
95	S: 2.0	0.1	0.2	0.1	0
	X: 8.4	0.16	0.3	0.14	0.1
	Ku: 14.0–16.0	0.4	0.7	0.4	0.2
	Ka: 27.5–29.5	1.2	3.0	0.8	0.4
	W: 78.0–79.0	7	18.0	4.0	2.4
99	S: 2.0	0.1	0.3	0.1	0
	X: 8.4	0.16	0.4	0.16	0.12
	Ku: 14.0–16.0	0.4	0.8	0.6	0.3
	Ka: 27.5–29.5	1.2	4.0	1.2	0.5
	W: 78.0–79.0	7	24.0	5.5	3.0

B. Earth-Based Antenna Pointing to the Moon

1. Antenna Noise Temperature. Signal propagation loss through the Moon's negligible atmosphere can be easily ignored. The brightness temperature of the Moon is mainly due to the surface reflection of the Sun's light and heating effects at microwave frequencies. Lunar surface temperatures measured at various frequencies are shown in Fig. 7. They have a weak dependence on frequency above 1.0 GHz and vary from about 140 K at the new Moon up to 280 K at the full Moon. This temperature is generally higher than the Earth's atmospheric noise temperature for a link with a high elevation angle. Since the Moon's radius is only about one fourth of the Earth's and there is a distance of 60 Earth radii between the Moon and Earth, the view angle of the Moon relative to the Earth is ±0.25 deg. Also, due to the inclination of the Moon relative to the ecliptic plane, the Moon is observed within ±5 deg in declination of the plane of the ecliptic, as shown in Fig. 8 [6,11,14]. Thus, relative to the equator, which is ±23.5 deg up and down relative to the ecliptic plane, the Moon has a declination range of ±28.5 deg.

Because the self-rotation period of the Moon is the same as its revolution period about the Earth, at any time the same lunar hemisphere is always viewed from Earth. Given a ±5-deg inclination of the Moon relative to the ecliptic plane, there is a maximum of 59 percent of lunar surface that can be seen from the Earth. The radio emission from the Moon is a result of the Sun's reflected emission, and very little radiation is radiated from the Moon itself as a blackbody emitter.

For the purpose of simplification, the ITU has used a fixed average temperature of 210 deg to model the Moon's surface brightness temperature when a 0.5-deg beamwidth of the antenna points to the Moon, between 1 and 100 GHz, as shown by line B in Fig. 9 [6]. Thus, at a higher (>10 deg) elevation angle, the Earth's atmospheric contribution, as compared to the Moon's noise temperature, can be neglected, as shown in Fig. 5. However, when an Earth-based antenna tracks the Moon at a very low elevation angle, the brightness temperature due to Earth's atmosphere can be higher than the Moon's brightness temperature. Thus, an actual temperature from our calculation (Fig. 5) should be used.

2. Noise Temperature Computation for an Antenna Pointing to a Blackbody. In this section, we will show a general methodology with which the antenna noise temperature can be calculated when it points to a blackbody (such as the Moon). Antenna noise temperature caused by blackbody

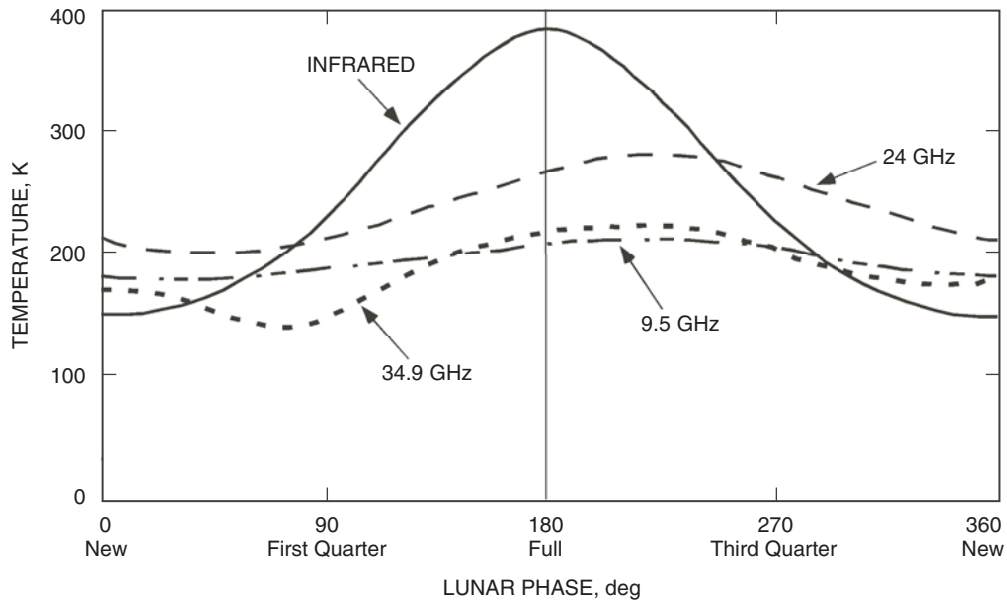

Fig. 7. Lunar temperature in kelvins as a function of lunar phase, showing the temperature variation, at infrared wavelengths and at frequencies of 9.5, 24.0, and 34.9 GHz. The temperatures are those of an equivalent blackbody radiator [11].

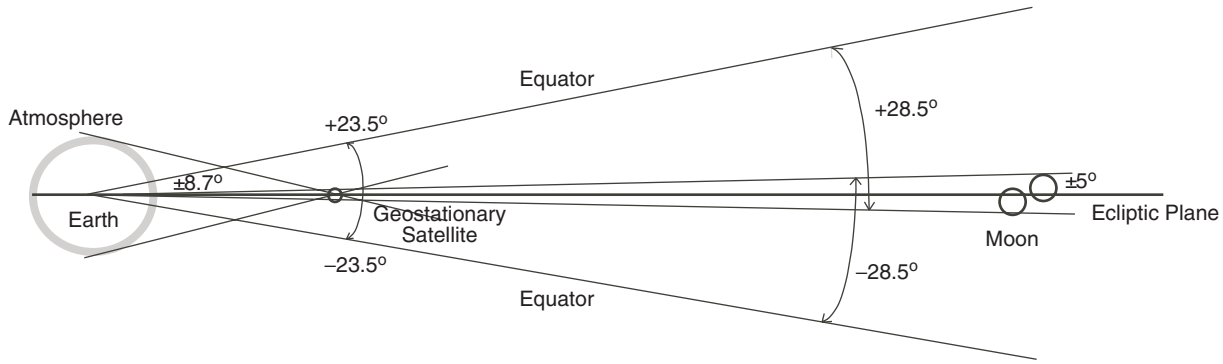

Fig. 8. Region of sky that is relevant for telecommunication with an Earth-based antenna and a satellite in geostationary orbit. The geometric view angle of the Moon relative to an Earth-based antenna is ±5 deg, while the solid Earth relative to a geostationary satellite is ±8.7 deg. The equatorial plane, which a geostationary satellite stays with, will have ±23.5 deg up and down relative to the ecliptic plane.

radiation greatly depends on beam coverage and the relative location of its boresight axis to the blackbody disk. However, because our final result has been normalized by the blackbody's temperature and disk size, it can be applied to any type of black bodies.

Here we will show a complete procedure for determining the noise temperature of an antenna when it points to a blackbody. This geometry and all the parameters used in this calculation are shown in Fig. 10. In this figure, a receiving antenna's half-power beamwidth (HPBW) relative to a circular blackbody is shown. There are two types of beams, HPBW $\ll D_\theta$ and HPBW $\gg D_\theta$, where D_θ is the angular diameter of the blackbody disk. The blackbody's radius is r_d, while the distance between the beam center and disk center is l_d. The distance between the receiving antenna and the blackbody is not important for this scenario because angular distances are used.

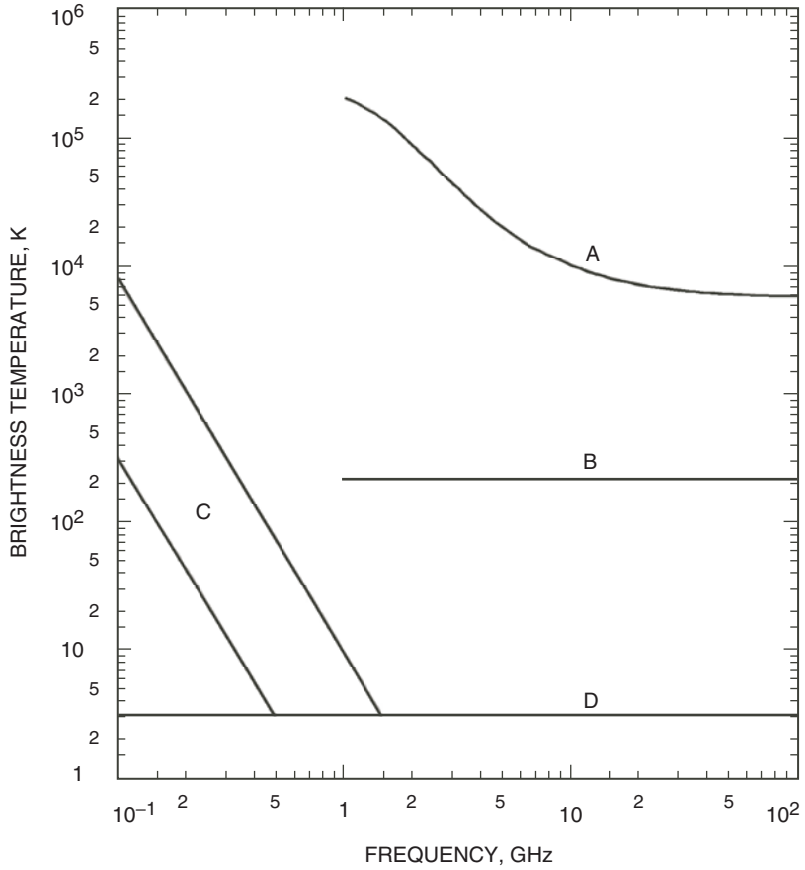

Fig. 9. All noises from extra-terrestrial sources. Line A is from a quiet Sun, while line B is from the Moon (all with a 0.5-deg beamwidth diameter). Galactic noise (C) and cosmic background (D) are also shown. Lunar emission is independent of the noise frequency [6].

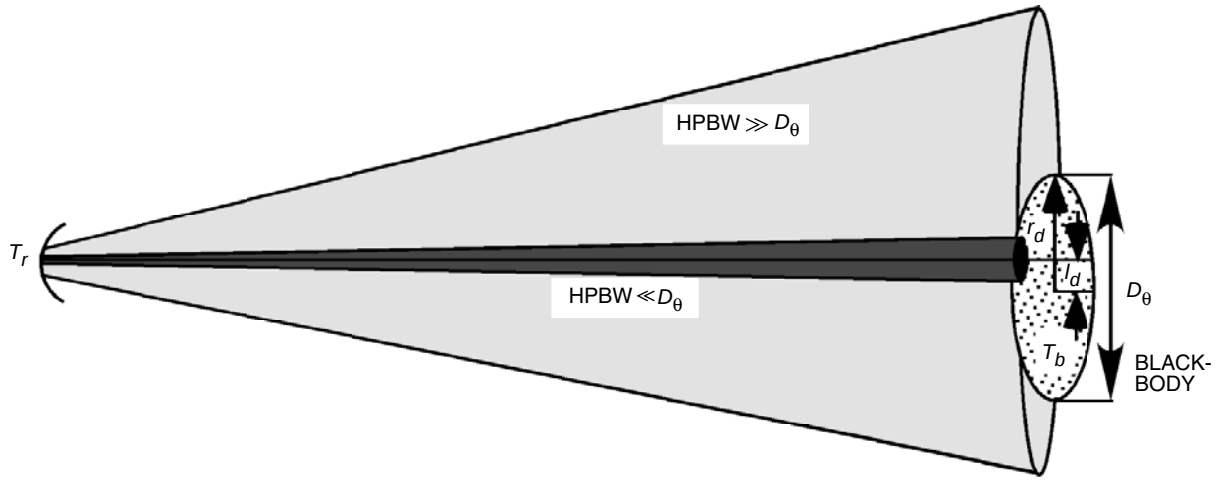

Fig. 10. Geometry of antenna beams with two types of beamwidths relative to a blackbody.

In most hot-body cases, the brightness temperature is assumed constant over the entire surface of the body, and the hot body radiates equally in all directions, i.e., the hot body is an omnidirectional radiator. The temperature increase due to blackbody radiation is then given by Eq. (15), which is reproduced here in a slightly different form:

$$\frac{T_{\text{incr}}}{T_b} = \frac{\int_{\text{disk}} G_r(\theta,\phi) T_b d\Omega}{\int_{4\pi} G_r(\theta,\phi) T_b d\Omega} \tag{18}$$

where T_{incr} is the temperature increase, T_b is the hot-body temperature (K), and $G_r(\theta,\phi)$ is the receiving antenna normalized power pattern when its boresight points to the blackbody. It should be understood that the integration in the numerator is over the solid angle of the blackbody disk only, and the integration in the denominator is over all space (4π).

The spacecraft is assumed to be tracked by a large antenna such as a DSN 34- or 70-meter-diameter antenna. The 34-meter antenna has its 3-dB beamwidth at about 0.5 deg, similar to the Moon's angular width at the Earth's surface, and the 70-meter antenna has a beamwidth smaller than 0.5 deg. When the spacecraft is near the Moon or in an orbit around the Moon, the receiving antenna may see part of the Moon within its 3-dB beamwidth, while the remaining part of the beam may be out of the Moon area on cold sky. Thus, using the Moon temperature as shown in Fig. 9 to perform a link analysis would yield a pessimistic result, i.e., the link may predict a supportable bit rate at the acceptable data margin that is lower than the actual Moon temperature seen by the antenna. Thus, to perform an accurate analysis of the system noise temperature increase due to the Moon, the following method is suggested.

To compute the results, the Bessel-function approximation of the normalized power pattern (including the main lobe and side lobes) of the antenna will be used:

$$G_{\text{Bes}}(\theta) = \left[\frac{2J_1\left(\frac{\pi D_a}{\lambda}\sin(\theta)\right)}{\frac{\pi D_a}{\lambda}\sin(\theta)} \right]^2 \tag{19}$$

where θ is the angle off antenna boresight, D_a is the antenna diameter, J_1 is the Bessel function of order 1, and λ is the associated wavelength. It should be noted that D_a and λ are in the same units. Substituting the above Bessel function approximation for the antenna gain pattern in the temperature increase fraction, Eq. (18), and integrating gives the results discussed in the following.

The above equations and procedures were programmed into a Microsoft Excel spreadsheet. Using this program, the ratios of increased system noise temperatures were generated, with the results as shown in Figs. 11 through 14. It should be noted that each of the four graphs are plotted (with the same parameter axis) for different groups of parameter values and axis ranges. Thus, a description of any one of these graphs should suffice to explain the remaining graphs. Figure 11 plots the normalized increased ratio in temperature, i.e., the left-hand side of Eq. (18), as a function of the blackbody-disk-center-to-beam-center distance, l_d, normalized to the disk radius, r_d. Thus, for an x-axis value of 0, the beam is centered on the blackbody disk. For an x-axis value of 1.0, the beam center is on the edge of the disk. The curve parameters are the ratios of the full 3-dB beamwidths of the antenna beam to the angular diameters, D_θ, of the blackbody disk. We can see that, as the antenna beam sizes increase from 1 to 10 percent relative to the disk diameter, HPBW/D_θ, the noise temperature increases less when the antenna beam is within the blackbody disk (that is, $l_d/r_d < 1.0$). This is due to the larger antenna beamwidth, which usually has a lower peak gain and a lower efficiency for detecting the noise temperature from a blackbody. It should be noted that the normalization of the abscissa is with respect to the disk radius, while the normalization of the curve parameter is with respect to the disk diameter.

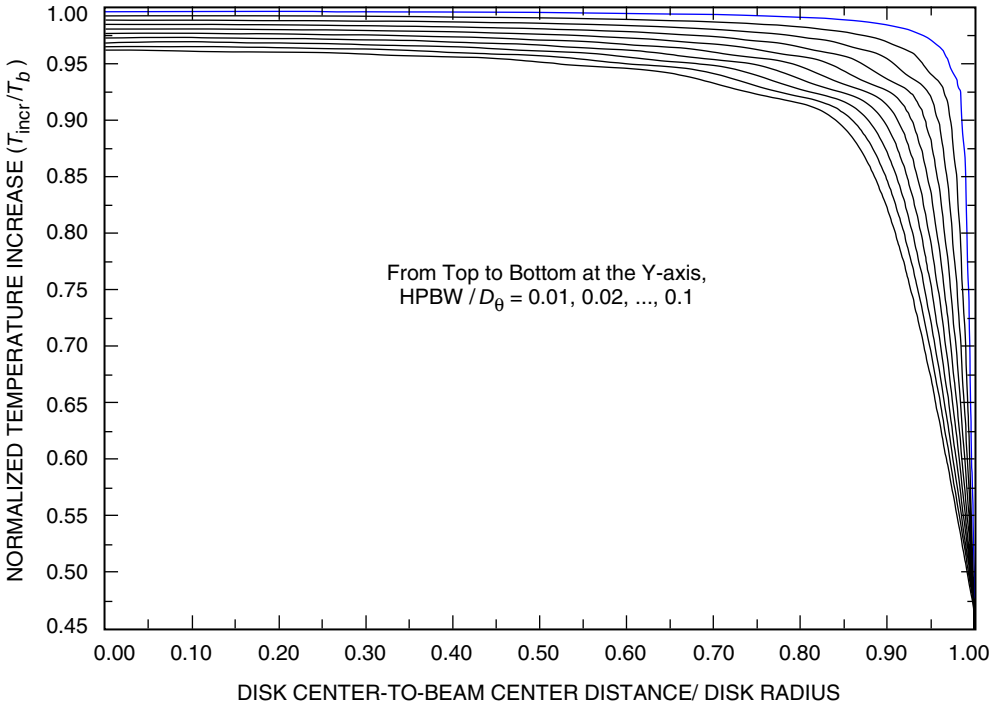

Fig. 11. Normalized temperature increase as a function of normalized distance from disk center when HPBW $\ll D_\theta$ **with the beam inside the disk.**

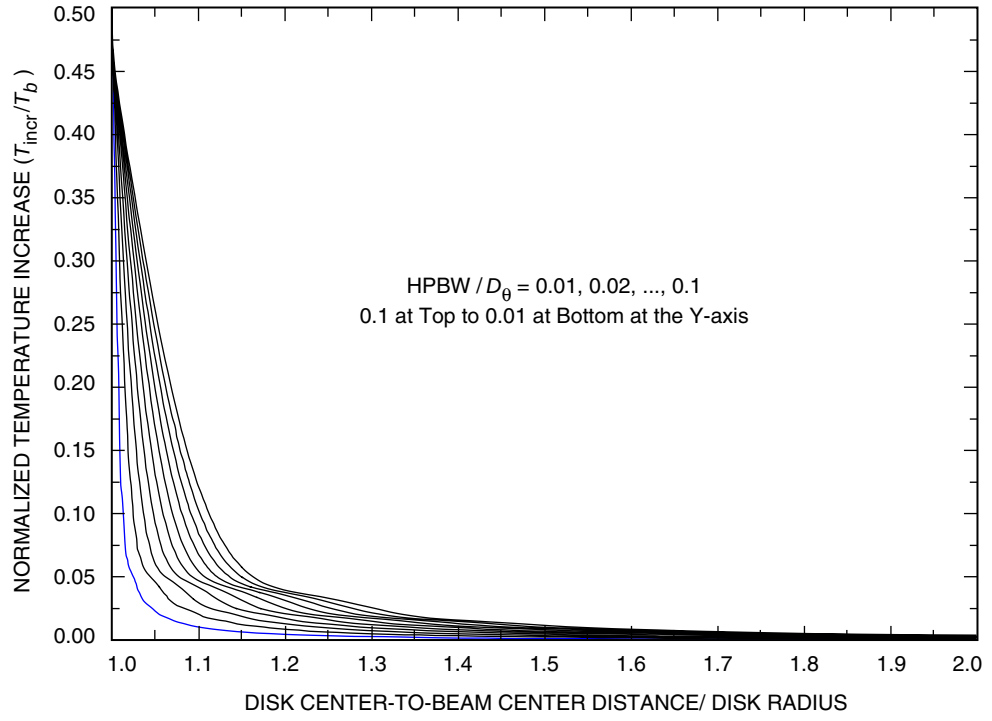

Fig. 12. Normalized temperature increase as a function of normalized distance from disk center when HPBW $\ll D_\theta$ **with the beam outside the disk.**

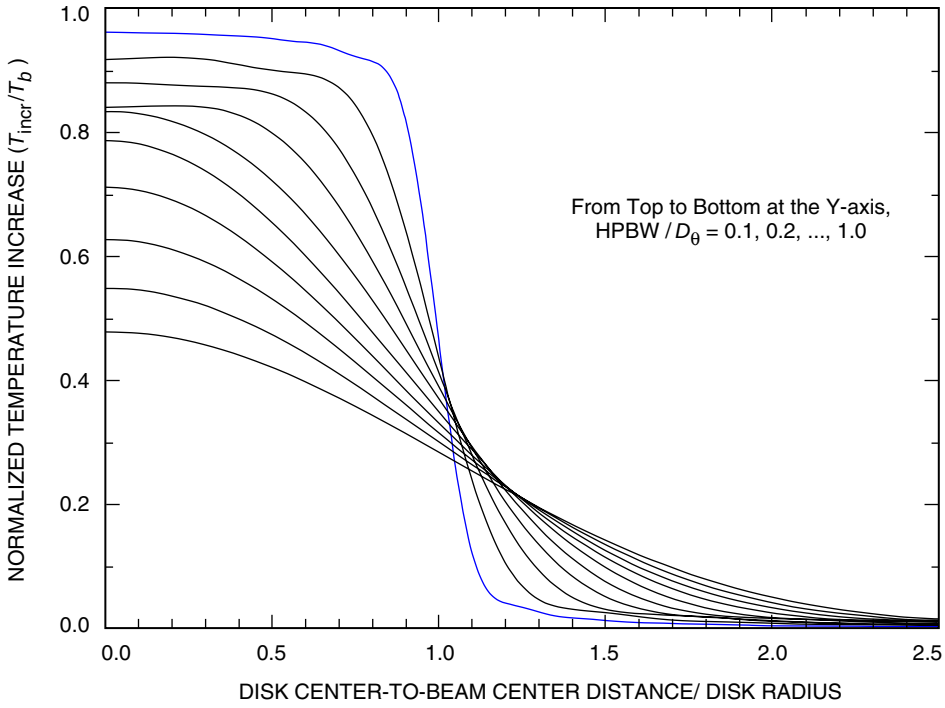

Fig. 13. Normalized temperature increase as a function of normalized distance from disk center when HPBW $\leq D_\theta$ **with the beam from the inside to the outside of the disk.**

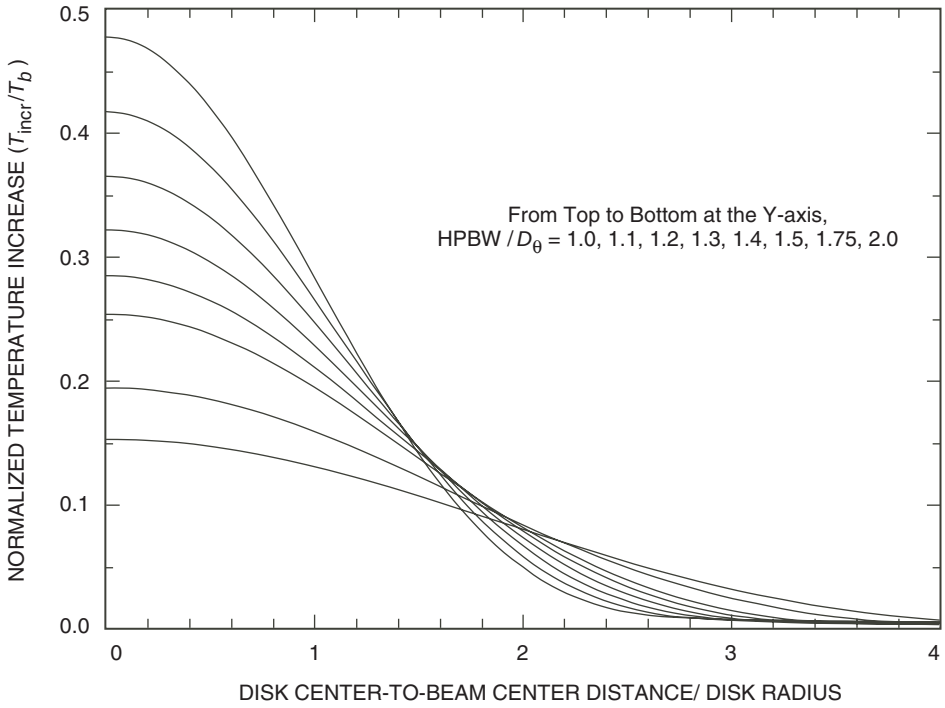

Fig. 14. Normalized temperature increase as a function of normalized distance from disk center when HPBW $\geq D_\theta$ **with the beam from the inside to the outside of the disk.**

In Fig. 11, the curve parameters range from 0.01 to 0.1 in steps of 0.01. For this figure, HPBW $\ll$ disk diameter (this applies a restraint on the distance between the receiver antenna and the blackbody) as the antenna beam center starts from the center of the disk and moves to the edge of the disk. Thus, most of the time, the antenna beam falls entirely inside the disk. In Fig. 12, the curve parameters also vary from 0.01 to 0.1 in steps of 0.01 and with HPBW $\ll$ disk diameter (D_θ), just as in the case shown in Fig. 11. However, this figure shows the beam center starting from the edge of the disk as it moves from the center of the disk up to one diameter of the disk or twice the radius of the disk. Thus, most of the time, the beam is entirely outside the disk. Figure 13 is similar to Figs. 11 and 12, with only parameter value changing from 0.1 to 1.0, when HPBW $\leq$ disk diameter (D_θ). The beam moves from the center of the disk to 2.5 radii. Thus, this figure shows the effects of the beam being entirely inside the disk as well as being entirely outside the disk. Figure 14 shows the fractional system noise temperature increase when the parameter value is varied from 1.0 to 2.0 in the indicated steps when HPBW $\geq$ disk diameter. The beam starts from the center of the disk and moves up to 4 times the radius of the disk or 2 times the diameter of the disk. In this case, since HPBW is greater than the disk diameter, some portion of the beam is always outside of the disk area.

As an example of the use of these figures, let the tracking antenna be a DSN 70-meter antenna. The half-power beamwidth of this antenna at the X-band frequency (8.450 GHz) is about 0.032 deg. Suppose the antenna is tracking a satellite with the center of the main lobe at the center of the Moon (i.e., the spacecraft is directly in front of the Moon while orbiting the Moon, as seen from the Earth). With an apparent Moon diameter of 0.5 deg as seen from the Earth, the value of the parameter of the graphs equals $0.032/0.5 = 0.064$ (HPBW $\ll D_\theta$). Since the antenna beam is focused at the center of the Moon, the value of the Moon-center-to-beam-center distance equals 0.

Figure 11 provides $T_{\text{incr}}/T_b = 0.988429$ for the parameter value of 0.064 and $T_{\text{incr}}/T_b = 0.972564$ for the parameter value of 0.07. Performing an interpolation, we obtain $T_{\text{incr}}/T_b = 0.974902$ for the desired parameter value of 0.064. Hence, to obtain the actual temperature increase, we need the Moon disk temperature, T_b. If the temperature, T_b, is 240 K, then the temperature increase at the DSN station processing the signals from the 70-meter station would be $240 \times 0.974902 = 233.9765$ K. It was noted that all the results derived earlier are for a receiving antenna efficiency of 100 percent. Hence, the efficiency of a 70-meter antenna, approximately 75 percent, must be multiplied to the above result to get the actual answer. Thus, the temperature increase becomes $233.9765 \times 0.75 = 175.482$ K. This result can also be applied to other cases.

3. Atmospheric Attenuation. For an Earth-based antenna pointing to the Moon, the atmospheric attenuation is exactly the same as that described in Section III.A.2 (the case of an Earth-based antenna pointing toward an orbiting spacecraft). Attenuation magnitude can be found in Fig. 6 and Table 1.

C. Geostationary Satellite Antenna Pointing to the Earth

1. Antenna Noise Temperature. For telecommunication using satellites in geostationary orbit, a limited part of the sky is of special interest, as illustrated in Fig. 8, with the corresponding range of declinations. The solid Earth surface (except its atmosphere) has a view angle of ± 8.7 deg relative to a geostationary satellite, which is at 6.6 Earth radii [8]. Thus, a geostationary satellite, which always stays inside the equatorial plane, can have an inclination angle as much as ± 28.5 deg relative to the Moon.

For the uplink, the Earth-viewing antenna observes the Earth's surface emission and atmospheric radiation. An Earth-coverage beam will receive the emissions from areas with varying land/ocean fractions within the field of view. Usually, the observed noise is a complex function of atmospheric and surface temperature, elevation angle, frequency, and antenna gain. For the Earth's surface, the land has a higher brightness temperature, while the sea has a lower brightness temperature in the main antenna beam. Upwelling brightness temperature due to Earth's atmosphere and surface radiation is shown in Fig. 15 as

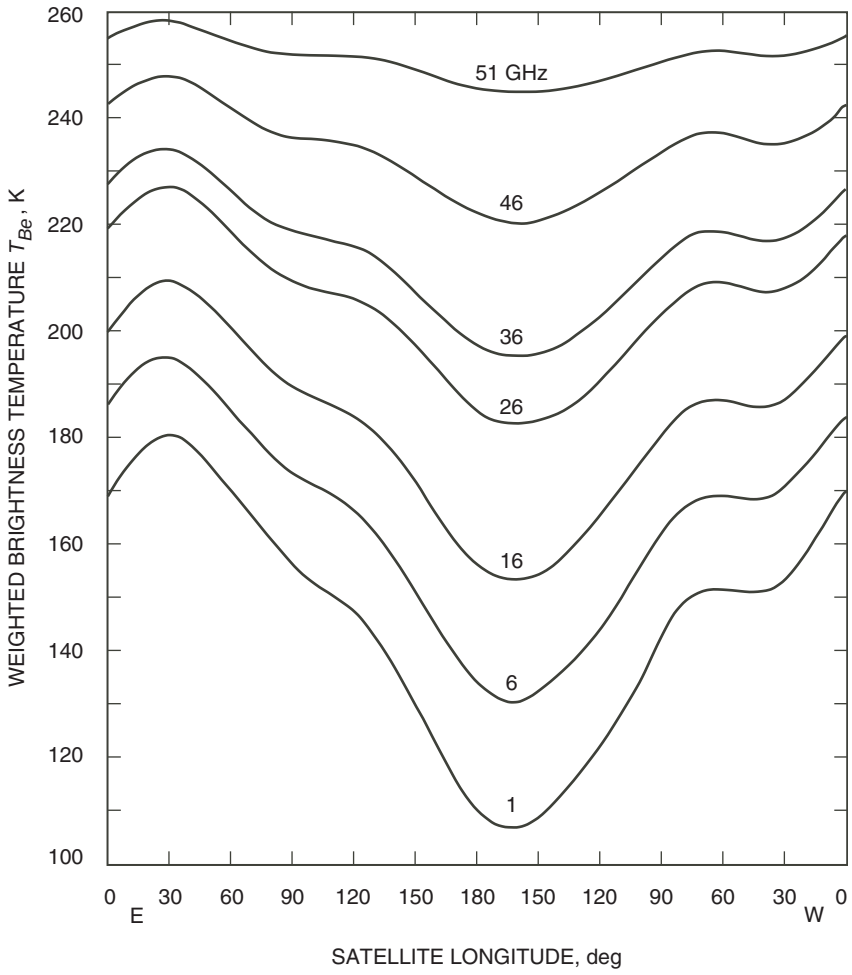

Fig. 15. Weighted brightness temperature as a function of longitude viewed from a geostationary satellite at frequencies between 1 and 51 GHz. Curves are for U.S. Standard Atmosphere with 2.5 g/cm^3 water vapor and 50 percent cloud cover. Surface parameters are stated in [8]. (Redrawn from [8].)

a function of the longitude of the satellite position. We can see that the brightness temperature varies with frequency and subsatellite longitude. The effects of varying land/ocean fractions viewed from different positions around the equator are quite evident. The lowest land fraction, 0.17 at 160°W, and the highest, 0.46 at 30°E, correspond to the lowest and highest observed brightness temperatures, respectively. The peak-to-peak brightness temperature variation around the equator ranges from 74 K at 1 GHz to 13 K at 51 GHz [8].

At other angles, a space-background brightness temperature of 2.7 K at frequencies above 3 GHz should be used for the integration. At the back lobe (if pointing to the Moon), a 210-K brightness temperature should be considered within a ±5 deg coverage.

2. Atmospheric Attenuation. For a geostationary satellite antenna pointing toward the Earth, the atmospheric attenuation is exactly the same as that of an Earth-based antenna pointing toward an orbiting spacecraft (see Section III.A.2). Attenuation magnitude can be found in Fig. 6 and Table 1.

D. Geostationary Satellite Antenna Pointing toward the Moon

1. Antenna Noise Temperature. Here we have assumed that the geostationary satellite can also point its antenna to the Moon. The minimum distance between the Moon and geostationary satellite is 53.4 Earth radii. The view angle of the Moon relative to a geostationary satellite is ±0.28 deg. When a geostationary spacecraft with a narrow beam (<0.5 deg) points to the Moon, the Moon's brightness temperature can be approximated at 210 K, between 1 and 100 GHz, as shown by line B in Fig. 9. Beyond this, the space-background brightness temperature has a constant value of approximately 2.7 K at frequencies above 3 GHz. For an accurate calculation, noise temperature increases for a geostationary satellite are similar to those shown in Sections III.B.1 and III.B.2 when its antenna points to the Moon. The only difference is that the back lobe of the antenna of a geostationary spacecraft may receive some upwelling radiations from Earth's atmosphere, as shown in Figs. 4 and 5 [8]. In general, these back-lobe effects can be neglected.

2. Atmospheric Attenuation. Since there is very little atmosphere in the space between a geostationary satellite and the Moon's surface, the effects of atmospheric attenuation for this link may be neglected.

E. Moon-Based Antenna Pointing toward Earth

1. Antenna Noise Temperature. Relative to the Moon, Earth has a view angle of $\tan^{-1}(1/60) \approx \pm 1$ deg, and considering the inclination of the Moon relative to the ecliptic plane, the Earth has a view angle of ±5 deg relative to a fixed Moon-based antenna. The viewing geometry is shown in Fig. 16 [6]. This case is basically similar to the case of a geostationary satellite antenna pointing toward the Earth (Section III.C.1). However, instead a ±8.7 deg view angle, as shown in Fig. 16, a smaller beam coverage angle (±5 deg) should be used for the integration. The weighted brightness noise temperatures, as a function of sub-longitude of the Moon, are shown in Fig. 15. At other angles, a space-background brightness temperature has a constant value of approximately 2.7 K at frequencies above 3 GHz. At its back lobe (if pointing to the Moon), a 210-K radiation from the Moon's surface should be considered for the side-lobe integration [6,11,14].

2. Atmospheric Attenuation. For a Moon-based antenna pointing toward the Earth, the atmospheric attenuation is exactly the same as that of an Earth-based antenna pointing toward an orbiting spacecraft (see Section III.A.2). Attenuation magnitude can be found in Fig. 6 and Table 1.

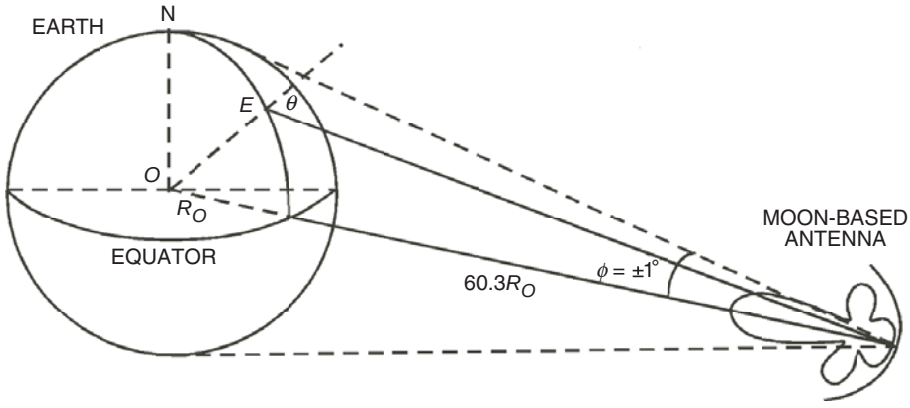

Fig. 16. Geometry for a Moon-based antenna viewing the Earth, where θ is the Moon's elevation angle relative to Earth's point E, r_o is the Earth's radius, and Earth has a ±1-deg view angle relative to the Moon.

F. Moon-Based Antenna Pointing toward a Geostationary Spacecraft

1. Antenna Noise Temperature. Here we have assumed that there is a telecommunication link between the Moon surface and a geostationary satellite, while Earth is in the background. Since the Earth is in the background, for this case the brightness noise temperature within a ±5 deg viewing angle is the same as the situation in Section III.E.1.

2. Atmospheric Attenuation. Because there is almost no air in the space between a geostationary satellite and the Moon's surface, there is very little atmospheric attenuation for this link (the same as in Section III.D.2).

IV. Summary

An analysis for an Earth–satellite–Moon telecommunication system has been performed. We find that uncertainties in two factors will affect the system's performance (or data transfer rate) after the carrier frequency is selected. They are the effective antenna gain and operating system noise temperature. For an Earth–satellite–Moon telecommunication system, the two factors are closely related to the atmospheric attenuation and brightness temperature. In this study, we have included all effects caused by atmospheric attenuation and noise temperature. Six cases of an Earth–satellite–Moon telecommunication link have been analyzed by taking into account atmospheric radiation and atmospheric attenuation.

In the SHF band, attenuations due to Earth's atmosphere include gaseous absorption, clouds and rain, and scintillation, etc., as shown in Table 1 and Fig. 6. Earth's brightness temperatures due to atmospheric radiation and surface emission for an upward-looking and a downward-looking antenna are also calculated and presented. The Moon's brightness temperatures due to its surface emissions were also modeled and presented. These brightness noise temperatures are functions of signal frequency, elevation angle, water vapor density, cloud liquid-water contents, percent of time availability, sub-longitudes of a geostationary satellite, and the Moon's lunar phase. All of this information has been presented and is illustrated in Figs. 2, 4–6, 8, 9, and 15.

It was shown that the receiving antenna noise temperature can be estimated by integrating its gain over the view angles of the pointed radiating sources, depending on the antenna gain pattern. In the majority of cases, this single brightness source has a very small view angle (<1 deg), and the antenna temperature is almost the same as the background brightness temperature. Otherwise, the integration will include all solid angles and the main-beam dominating factors of the receiving antenna. This study provides a general solution in accurately computing antenna noise temperature caused by a blackbody in the SHF band. This procedure can be applied to any receiving antenna and blackbody, because the results are independent of the antenna size, blackbody size, and temperature. The final results are presented as a ratio of antenna noise temperature relative to the blackbody temperature as a function of relative beam size versus beam off-center distance to the blackbody disk, which facilitates the calculation of noise temperature for an Earth-based antenna pointing to the Moon.

Acknowledgment

The authors would like to thank Charles Ruggier for his reviewing of this article.

References

[1] "Attenuation by Atmospheric Gases," Recommendation ITU-R P.676, International Telecommunications Union, Geneva, Switzerland, 1999.

[2] "Attenuation due to Clouds and Fog," Recommendation ITU-R P.840, International Telecommunications Union, Geneva, Switzerland, 2003.

[3] J. W. Waters, "Absorption and Emission by Atmospheric Gases," in *Astrophysics-Part B: Radio Telescopes*, vol. 12, *Methods of Experimental Physics*, M. L. Meeks, ed., New York: Academic Press, pp. 142–176, 1976.

[4] H. J. Liebe, "Modelling Attenuation and Phase of Radio Waves in Air at Frequencies below 1000 GHz," *Radio Science*, vol. 16, pp. 1183–1199, 1981.

[5] F. T. Ulaby, R. K. Moore, and A. K. Fung, "Microwave Interaction with Atmospheric Constituents," in *Microwave Remote Sensing: Active and Passive*, vol. 1, *Microwave Remote Sensing Fundamentals and Radiometry*, F. T. Ulaby et al., eds., Reading, Massachusetts: Addison-Wesley Publishing Company, Inc., pp. 256–290, 1981.

[6] "Radio Noise," Recommendation ITU-R P.372-8, International Telecommunications Union, Geneva, Switzerland, 2003.

[7] "Radio Emission from Natural Source in the Frequency Range above 50 MHz," Report 720-2, International Radio Consultative Committee, International Telecommunications Union, Geneva, Switzerland, 1986.

[8] E. G. Njoku and E. K. Smith, "Microwave Antenna Temperature of the Earth from Geostationary Orbit," *Radio Science*, vol. 20, pp. 591–599, 1985.

[9] "Use of Radio-Noise Data in Spectrum Utilization Studies," Recommendation 508, International Radio Consultative Committee, International Telecommunications Union, Geneva, Switzerland, 1978.

[10] C. T. Stelzried, *The Deep Space Network—Noise Temperature Concepts, Measurements, and Performance*, JPL Publication 82-33, Jet Propulsion Laboratory, Pasadena, California, September 15, 1982.

[11] J. D. Kraus, *Radio Astronomy*, 2nd ed., Powell, Ohio: Cygnus-Quasar Books, 1986.

[12] C. Ho, S. Slobin, M. Sue, and E. Njoku, "Mars Background Noise Temperatures Received by Spacecraft Antennas," *The Interplanetary Network Progress Report 42-149, January–March 2002*, Jet Propulsion Laboratory, Pasadena, California, pp. 1–15, May 15, 2002. http://ipnpr/progress_report/42-149/149C.pdf

[13] CCIR, "Attenuation by Atmospheric Gases," Report 719-2, in *Propagation in Non-ionized Media, Recommendation and Report of the CCIR*, vol. V, International Radio Consultative Committee, International Telecommunications Union, Geneva, Switzerland, pp. 167–176, 1986.

[14] M. I. Skolnik, *Radar Handbook*, Chapter 39, New York: McGraw-Hill Book Co., pp. 39–24, 1970.